Stress analysis of unsaturated soil based on the 'driest curve'

Analyse de tensions de sols non-saturés basée sur la 'condition la plus sèche'

D. Karube – *Department of Civil Engineering, Kobe University, Japan*

ABSTRACT: The paper proposes that, in the constitutive equations for unsaturated soils, the isotropic stress component should be decomposed into two parts: the compressive stress transmitting through the soil skeleton and the internal normal stress at interparticle contact points. These two parts can be evaluated individually by introducing a new concept called 'driest curve' which is defined by the soil-water characteristic curve corresponding to the driest condition. The application of this concept is realized by extending 'Cambridge model for saturated clays' to the unsaturated conditions. The extended model can well explain the results of triaxial tests on saturated and unsaturated soils.

RESUME: Cet article propose que, dans les équations constitutives pour des sols non-saturés, la composante isotrope de tension doit être décomposée en deux parts: la tension compressive qui se transmet par la squelette de sol et la tension normal interne aux contacts des particlues. Ces deux parts peuvent être evaluées separément par l'introduction d'un concept nouvel qui s'appelle 'la courve la plus sèche'; La courve est définie par la courve caractéristique de sol-eau correspondante à la condition la plus sèche. L'application de ce model est réalizée par étendant 'le model Cambridge pour des arigiles saturées' pour des sols non-saturés. Le model étendu peut bien expliquer les résultats des essais triaxiaux sur des sols saturés et non-saturés.

1 INTRODUCTION

Bishop's effective stress equation extended to unsaturated state failed to explain the collapse phenomenon. Matyas and Radhakrishna(1968) conducted a one dimensional compression test on unsaturated soil and got a family of void ratio contour lines on the plane of suction vs. net stress $(\sigma - u_a)$, however, a plastic compression induced by increasing suction was not investigated. Karube(1987) developed an equation of plastic isotropic compression, but it was not applicable to the wet state, too. Though Alonso et al.(1990) introduced a yield surface for increasing suction, obtained constitutive equation was complicated. Kohgo et al.(1993) defined an effective stress of Bishop's type and, in order to cover its defect in the plastic compression, they introduced an empirical State Boundary Surface. But the applicability of developed constitutive equation must be limited because the hysteresis between suction and induced suction stress was not considered.

Karube and Kato(1994) pointed out that the role of meniscus water in constitutive equation is different from pore water filling small bulks among soil skeletons and they developed an equation of plastic compression for a given volume ratio of meniscus water to bulk water. But the method for estimating the ratio of them in a soil mass had not been developed. Wheeler and Karube(1995) proposed the method of estimation based on the "driest curve", which is a soil-water characteristic curve corresponding to the driest condition.

2 NORMAL STRESS COMPONENTS IN UNSATURATED SOIL

In a saturated soil mass, normal stress transmitting through the soil skeleton is effective stress, σ'. On the other hand, interparticle normal stress, σ^* is sum of the effective stress and the internal(intrinsic) stress such as Coulomb's force, σ_ℓ, i.e.,

$$\sigma^* = \sigma' + \sigma_\ell \tag{1}$$

As soil is a frictional material, the shear strength is given as;

$$\tau_f = \sigma^* \tan\phi^* \tag{2}$$

where, ϕ^* denotes interparticle frictional modulus, and cohesion is ignored here for simplicity.

However, the equation of shear strength is given, in general, in terms of effective stress as,

$$\tau_f = \sigma' \tan\phi' \tag{3}$$

Equating Eq(2) and Eq(3),

$$\frac{\tan\phi'}{\tan\phi^*} = \frac{\sigma^*}{\sigma'} = 1 + \frac{\sigma_\ell}{\sigma'} = (1+\alpha) \tag{4}$$

where $\alpha = (\sigma_\ell / \sigma')$.

Eq(4) means the internal normal stress, σ_ℓ is generated in proportion to acting effective stress, σ'.

As for the compressibility of a soil mass, coefficient of volume change, m_v is defined as,

$$m_v = (dv / dp') \tag{5}$$

where, v: volumetric strain, p' : average effective stress.

In the normally consolidated state, volumetric strain is given as

$$v = \frac{\lambda}{1+e_0} \log \frac{p'}{p'_0} \tag{6}$$

$$\therefore \text{ Rigidity} = \frac{1}{m_v} = \frac{dp'}{dv} = \frac{1+e_0}{\lambda} p' \tag{7}$$

where, λ : compression index.

Though Eq(7) means that the rigidity of soil is in proportion to effective stress, it is the interparticle stress to make soil rigid. Therefore,

$$\frac{1}{m_v} = \frac{dp'}{dv} = \frac{1+e_0}{\lambda^*} p^* \tag{8}$$

$$\therefore \quad \frac{\lambda^*}{\lambda} = \frac{p^*}{p'} = 1 + \frac{p_\ell}{p'} = (1+\alpha) \tag{9}$$

where, p^*: average interparticle stress, λ^*: compression index corresponding to p^*, $p_\ell = p^* - p'$: average internal stress.

Eq(9) means the internal stress is generated in proportion to effective stress, again, and which is the reason why the principle of effective stress is valid.

On the other hand, Fig.1 is a conceptual figure of unsaturated soil. The outer frame of broken line denotes a soil element, of which cross sectional area is A. The pore water is considered to exist in three states. The adsorbed water is fixed on the surface of soil particles as a solid and has no pore water pressure. The bulk water fills some pores among soil skeletons just like as the pore

water in saturated soil. The meniscus water surrounds every contact point of soil particles which is not covered by the bulk water. The pore water pressures of bulk water and meniscus water are the same value, u_w. Pore air occupies the remaining pore and pore air pressure is u_a, which is higher than u_w. The difference of pore pressure is called as suction, s, here, i.e.,

$$u_a - u_w = s \tag{10}$$

A wavy surface, x-x, shown by a dotted line crosses the element through contact points of soil particles. The projected area to the cross section is A_a for pore air, A_m for meniscus water and A_b for bulk water: i.e.,

$$A = A_a + A_m + A_b \tag{11}$$

The relative areas are,

$$\chi_A = (A_a / A),\ \chi_b = (A_b / A),\ \chi_m = (A_m / A) \tag{12}$$

The total stress, p_T, interparticle stress, p^*, internal stress, p_ℓ, bulk stress, p_b, meniscus stress, p_m, suction stress p_s and net stress, p are defined as,

$$p_T = \frac{\sum P_{Ti}}{A},\quad p^* = \frac{\sum P_i^*}{A},\quad p_\ell = \frac{\sum P_{\ell i}}{A} \tag{13}$$

$$p_b = \chi_b \cdot s,\quad p_m = \chi_m \cdot s,\quad p_s = (\chi_b + \chi_m)\cdot s = p_b + p_m \tag{14}$$

$$p = p_T - u_a \tag{15}$$

The force acting on the soil element from upper surface to wavy surface are in equilibrium as,

$$\sum P_{Ti} + \sum P_{\ell i} = \sum P_i^* + A_a u_a + A_b u_w + A_m u_w$$

$$\therefore p^* = p + p_b + p_m + p_\ell = (p_T - u_a) + \chi_b \cdot s + \chi_m \cdot s + p_\ell \tag{16}$$

Because the terms $[p_m + p_\ell]$ in Eq(16) are the internal stresses which are canceled out with a part of interparticle stress, p^* at each contact point, the stress acting on soil skeleton, in other words, the stress transmitting through soil skeleton like as effective stress in saturated soil, is

Skeleton stress: $p' = p + p_b = (p_T - u_a) + \chi_b \cdot s$ (17)

As for the interparticle stress,

$$p^* = p' + p_\ell + p_m = (1+\alpha)p' + p_m$$

$$\therefore p^* \cong (1+\alpha)(p' + p_m) \tag{18}$$

3 DRIEST CURVE

The coefficients χ_b and χ_m in Eq(12) should be a function of the volume of bulk water and meniscus water, respectively. The following functions are assumed here as,

$$\chi_b = S_{rb} / (1 - S_{r0}) \tag{19}$$

$$\chi_m = S_{rm} / (1 - S_{r0}) \tag{20}$$

where, S_{rb}, S_{rm} and S_{r0} denote the volume of bulk water, meniscus water and adsorbed water converted into the fraction of degree of saturation, i.e.,

$$S_r = S_{rb} + S_{rm} + S_{r0} \tag{21}$$

where, S_r denotes the degree of saturation of a soil mass.

A new concept called the "driest curve" is introduced to estimate the fractions of S_r. The driest curve is a soil-water characteristic curve which retains no bulk water, i.e., of which

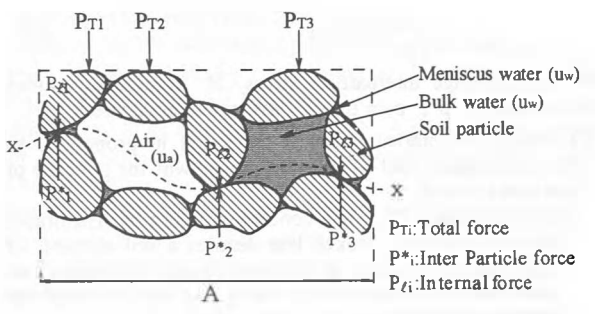

Fig.1 Acting forces in unsaturated soil.

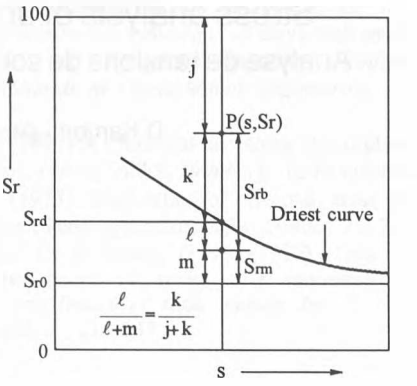

Fig.2 Estimation of Sr fractions.

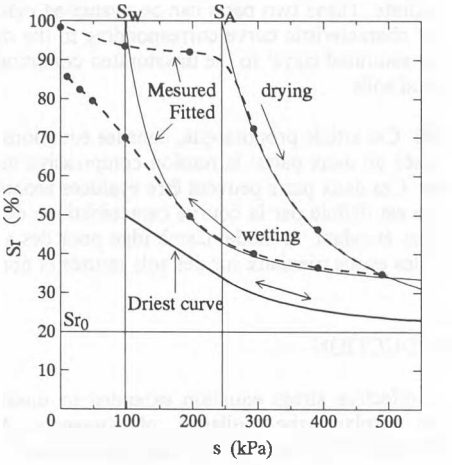

Fig.3 Determination of the Driest Curve.

pore water is composed from adsorbed water and meniscus water, therefore it indicates minimum value of S_r for given suction, s.

A point P(s, S_r) in Fig.2 denotes the current state of given soil and the curve is the driest curve. If a meniscus contacts bulk water, it is absorbed to bulk water. Therefore the bulk water fraction S_{rb} at P is larger than $(S_r - S_{rd}) = k$ and the meniscus water fraction S_{rm} is smaller than $(S_{rd} - S_{r0}) = (\ell + m)$. So following equations are proposed,

$$S_{rb} = \frac{S_r - S_{rd}}{1 - S_{rd}} \cdot (1 - S_{r0}) \tag{22}$$

$$S_{rm} = S_r - S_{rb} - S_{r0} \tag{23}$$

The driest curve and the fraction of adsorbed water, S_{r0} are obtained by Brooks and Corey's experimental equation fitted to soil-water characteristic curve of given soil. The broken lines in Fig.3 show the drying and wetting curves of the sample tested in this study, and thin fitting curves are Brooks and Corey's equations, which are

Drying curve: $$\frac{S_r - S_{r0}}{1 - S_{r0}} = \left(\frac{s_A}{s}\right)^{\lambda'} \tag{24}$$

Wetting curve: $$\frac{S_r - S'_{r0}}{1 - S'_{r0}} = \left(\frac{s_w}{s}\right)^{\lambda} \tag{25}$$

Equation of the driest curve is proposed as below,

$s \geq s_A$: $$\frac{S_{rd} - S_{r0}}{1 - S_{r0}} = \left(\frac{s_w}{s}\right)^{\lambda} \tag{26a}$$

$s_w < s < s_A$: $$\frac{S_{rd} - S_{r0}}{1 - S_{r0}} = \left(\frac{s_A}{s_w}\right)^{\lambda}\left[\frac{\lambda}{s_A} \cdot s + (1 - \lambda)\right] \tag{26b}$$

where, S_{rd} means S_r of the driest curve. S_{r0}, S'_{r0}, λ and λ' are

experimental constants decided by curve fitting. s_A and s_w are called as air entry value and water entry value, respectively, and these are decided by curve fitting, too. Thick curve and it's extrapolation line below the wetting curve show the driest curve proposed.

Finally stresses induced by suction are given by the following equations,

$$p_s = \frac{S_r - S_{r0}}{100 - S_{r0}} \cdot s \tag{27}$$

$$p_b = \frac{S_r - S_{rd}}{100 - S_{rd}} \cdot s \tag{28}$$

$$p_m = p_s - p_b \tag{29}$$

where S_{rd} is given by Eq(26a) and (26b).

4 ISOTROPIC COMPRESSION

The rigidity of saturated soil is given by Eq(8) and (9) as,

$$\frac{dp'}{dv} = \frac{1+e_i}{\lambda(1+\alpha)} p^* \tag{30}$$

where, p' : effective stress or skeleton stress
p^* : interparticle stress
$\alpha = (p_\ell / p')$, p_ℓ : internal stress
e_i : void ratio at zero strain

As for unsaturated soil, approximate interparticle stress is given by Eq(18), therefore

$$\frac{dp'}{dv} = \frac{1+e_i}{\lambda}(p' + p_m) \tag{31}$$

When plastic strain is considered, Eq(31) becomes,

$$\frac{dv^p}{dp'} = \frac{\lambda - \kappa}{1+e_i} \frac{1}{p' + p_m} \tag{32}$$

where, κ : swelling index.

Assuming that plastic volumetric strain is defined by stress state, i.e., a state boundary surface can be defined in $e \sim p' \sim p_m$ space, Eq(32) is integrated as,

$$v = \frac{\lambda - \kappa}{1+e_i} \log(p' + p_m) + C \tag{33}$$

If the initial yield function is defined as,

$$p' = p'_{y0} + a \cdot p_m \tag{34}$$

where, p'_{y0} : p' at $p_m = 0$, a: slope of yield function to p_m axis $(a \geq 0)$.

$$v^p = \frac{\lambda - \kappa}{1+e_i} \log \frac{p' + p_m}{p'_{y0} + (a+1)p_m} \tag{35}$$

The contour lines of plastic volumetric strain are given by,

$$p_m = \left[\frac{1}{(a+1)H - 1}\right] p' - \left[\frac{H}{(a+1)H - 1}\right] p'_{y0} \tag{36}$$

where,

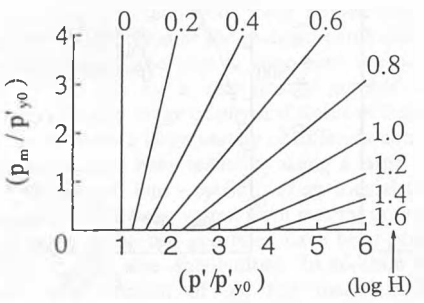

Fig.4 Family of loading curves.

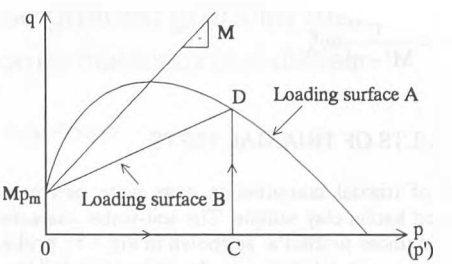

Fig.5 Loading surfaces.

$$H = \exp\left[\left(\frac{1+e_i}{\lambda - \kappa}\right) v^p\right] = \frac{p' + p_m}{p'_{y0} + (a+1)p_m} \tag{36}$$

Fig.4 shows Eq(36) in which a=0.

5 EXTENDED CAMBRIDGE CLAY MODEL

Original Cambridge Clay Model is extended to unsaturated state to realize the application of proposed theory. The original model applies to triaxial compression. Energy equation is rewritten for unsaturated soil as,

$$q = M^* p^* - p'(dv^p / d\varepsilon) \tag{37}$$

where, M^* denotes (q / p^*) at critical state, $\varepsilon = (2/3)(\varepsilon_a - \varepsilon_r)$.

Substituting M^* and p^* to M and p using Eq(4) and (18), Eq(37) becomes,

$$q = M(p' + p_m) - p'(dv^p / d\varepsilon) \tag{38}$$

where, M denotes (q / p') at critical state.

Applying the normality rule, the loading function is obtained as,

$$\frac{q}{M} = -p' \log \frac{p'}{p'_0} + p_m \left(1 - \frac{p'}{p'_0}\right) \tag{39}$$

where, p'_0: p' at $q = 0$.

The loading surface A in Fig.5 shows Eq(39). The equation of plastic volumetric strain during axial compression is obtained by equating p'_0 in Eq(39) with p' in Eq(35). The approximate equation at a=0 is as follows,

$$v^p = \frac{\lambda - \kappa}{1+e_i} \left\{ \log \frac{p' + p_m}{p'_{y0} + p_m} + \log \frac{(p'_{y0} + p_m)^2 + \frac{q}{2M}(p' - p_m)}{(p'_{y0} + p_m)^2 - \frac{q}{2M}(p' + p_m)} \right\} \tag{40}$$

The shear strain increment during axial compression is given by the following equation, which comes from Eq(38),

$$d\varepsilon = \frac{p' dv^p}{M(p' + p_m) - q} \tag{41}$$

where, dv^p is given by the total differential calculus of Eq(40).

It is often observed that the soil of low degree of saturation indicates a heavy dilatancy. To correspond to the dilatant behavior the extended Cam.Clay Model is re-extended by adding dilatant term, which is shown the loading surface B in Fig.5, that is,

$$dv^p = dv^p_A + dv^p_B \tag{42}$$

where, dv^p_A coincides with v^p given by Eq(40). On the other hand, dv^p_B is assumed as following function for simplicity,

$$dv^p_B = -\frac{M' - M}{M' - \eta'} dv^p_A \tag{43}$$

where, $\eta' = (q - Mp_m)/p'$ (44)

$$M' = (\eta')_f \tag{45}$$

Therefore volumetric and shear strain increment are given, respectively, as,

$$dv^p = \left(1 - \frac{M' - M}{M' - \eta'}\right) dv^p_A \tag{46}$$

$$d\varepsilon = \frac{1}{M' - \eta'} dv_A^p \qquad (47)$$

6 RESULTS OF TRIAXIAL TESTS

Series of triaxial compression tests were performed on initially saturated kaolin clay sample. The soil-water characteristic curve is obtained under p=20kPa, as shown in Fig.3 by broken line and the driest curve was calculated as shown by thick full line. Fig.6 shows the results of isotropic compression process, in which suction was kept constant value as indicated in Fig.7. Some specimens were loaded up to s=490kPa prior to isotropic compression. The data in Fig.6(a) are plotted in a form of Eq(35), on the other hand, abscissa of Fig.6(b) is log p. It can be seen that Eq(35) is valid. The axial compression process was performed under drained and strain controlled conditions. Fig.7 shows the failure stresses. Excess strength of unsaturated specimens comes from the suction stress and heavy dilatancy. Fig.8 shows the stresses at dilatancy rate is zero, when energy equation, Eq(38) becomes,

$$q = M(p' + p_m) + p'(dv^e/d\varepsilon) \qquad (48a)$$

Because the swelling index κ of tested sample is very small, second term in right side can be ignored compared with first term. Therefore

$$q \cong M(p' + p_m) = M(p + p_s) \qquad (48b)$$

where, $p = p_T - u_a$, and p_s is given by Eq(27).

Fig.8 shows the validity of Eq(48b)

Fig.9 is a example of calculated stress-strain curve based on Eq(46) and (47). Used soil parameters are summarized in Table 1. Because of simple dilatancy function, Eq(43), calculated curves show no strain softening, however, fitting is good in small shear strain range.

7 CONCLUSIONS

It has been assumed that pore water concentrates at the contact points of soil particles forming meniscus. It is true in a soil compacted dry of optimum, however, the fact that a given soil can have various degrees of saturation under constant suction implies the presence of bulk water occupying some bulk among soil skeletons.

In this paper, the pore water is classified into adsorbed water, bulk water and meniscus water, and a method for estimating the volume of each fraction using the driest curve is proposed. The action of each fraction of water is explained and introduced into an equation of isotropic compression and Cambridge Clay Model extended to unsaturated state. A few experimental evidences are shown, too. It is emphasized that the mechanical behavior of unsaturated soil should be studied on the plane of suction ~ degree of saturation.

The author wishes to acknowledge the discussions of Dr. M. Shimizu of Tottori University and Dr. S. Kato of Kobe University.

REFERENCES

Alonso, E.E., Gens, A. and Josa, A. 1990. A constitutive model for partially saturated soils, *Géotechnique* 40: 405-430.

Karube, D. 1987. Basic stress-strain relations of unsaturated soil. *Proc. 8th ARC-SMFE*. 49-52.

Karube, D. & Kato, S. 1994. An ideal unsaturated soil and the Bishop's soil. *Proc. 13th ICSMFE*: 43-46.

Kohgo, Y., Nakano, M. & Miyazaki, T. 1993. Verification of the generalized elastoplastic model for unsaturated soils. *Soils and Foundations* 33(4): 64-75.

Matyas, E.L. & Radhakrishna, H.S. 1968. Volume change characteristics of partially saturated soils. *Géotechnique* 18: 432-448.

Wheeler, S.J. & Karube, D. 1995. State of the art report - Constitutive modeling. *Proc. 1st IC on Unsaturated Soils* (to be published).

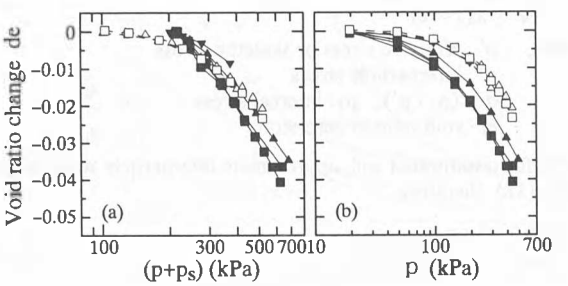

Fig.6 (a) de vs log(p+p_s) (b) de vs log p.

Table1. Parameters for calculations.

Parameter		Remarks
e_i	0.996	at specimen preparation
M	1.333	from saturated series
λ	0 .0459	
κ	0.0093	
S_{r0}	17.14%	Estimated from experiment
S_r	39.08%	Average during axial comp.
p	498kPa	Test conditions
s	294kPa	
p_b	48.2kPa	Calculated from S_{r0}, S_r, s
p_m	30.6kPa	
M'	1.822	Measured

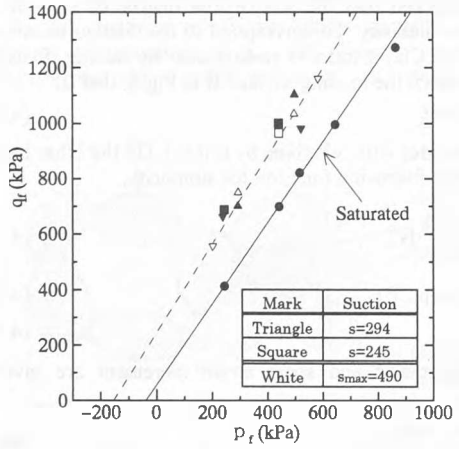

Fig.7 Failure stress.

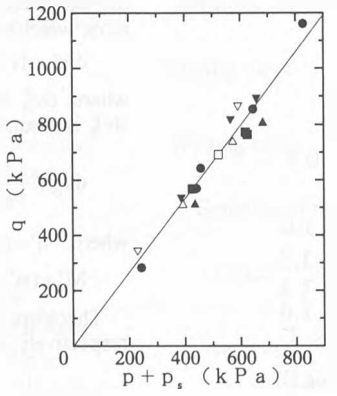

Fig.8 Stress at (dv/d ε)=0.

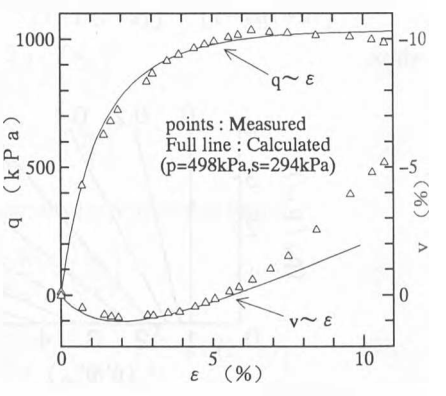

Fig.9 Measured and calculated stress-strain relations.